Progress In Electromagnetics Research B, Vol. 60, 259–274, 2014

Effects of Resonance-Based Phase Shifters on Ka-Band Phased Array Antenna Performance for Satellite Communications

Mehrbod Mohajer*, Mohammadsadegh Faraji-Dana, and Safieddin Safavi-Naeini

Abstract—Phase shifters are the key components of phased array systems which provide a low-profile solution for Ka-band satellite communications. In the transmitting mode, it is crucial for the phased array antenna system to meet the standard radiation masks, and any imperfections of phase shifters can yield into radiation mask violation. In this paper, we present the analytical approach to model the non-linear phase-frequency characteristics of Resonance-Based phase shifters, which constitute one of the most widely used class of phase shifters for Ka-band satellite communications. Furthermore, it has been investigated how the phase-frequency response non-linearity affects the phased array radiation patterns, gain, and the beam pointing direction. The simulation results show that, depending on the phase shifter phase-frequency response profile, the radiation mask satisfaction is an important factor in determining the system bandwidth.

1. INTRODUCTION

In recent years, the high potential of the Ka-band satellite communications has led to huge interest in this range of frequencies for low-cost, low-profile, and high performance land-mobile terminals (Satcom On-The-Move). Meanwhile, phased array systems provide a feasible solution for continuous tracking of the satellite directions in a fast and accurate manner. Hence, low-profile and low-cost two-way Ka-band phased array systems have been the centre of attention in a number of research programs [1–8].

One of the important challenges involved in the two-way Ka-band phased array system design is to meet the radiation mask requirements forced by satellite communication standards for transmitting mode of land-mobile terminals. Note that the radiation mask must be satisfied for the entire range of beam scanning angles. Since the beam scanning is performed by phase shifters, it is crucial to investigate how the gain and radiation pattern of the phased array will be affected by the nonlinearity of phase shifter phase-frequency response. Also, in this class of applications in addition to all other requirements, the size of the phase shifting device and its compatibility with low cost planar technologies are among crucial considerations. For Ka-band transmitters, it will be shown that the antenna element cell size should be about $0.5\,\text{cm} \times 0.5\,\text{cm}$, and 360 degree phase shifting is required for each antenna element in order to perform accurate beam-scanning without any mask violation. The Resonance-Based phase shifters are among the most promising and widely used structures which meet these requirements. A comprehensive survey on different types of phase shifters is performed to clarify why Resonance-Based phase shifters are among the most optimal choices for Ka-band communications. Generally, there are two types of phase shifters, namely Digital and Analog phase shifters. Due to the quantization errors of Digital phase shifters, it may not be possible to obtain sufficient phased array beam pointing resolution. For instance, let us consider an n-bit digital phase shifter which results in the minimum phase steps of

Received 9 June 2014, Accepted 5 August 2014, Scheduled 16 August 2014

* Corresponding author: Mehrbod Mohajer (mmohajer@uwaterloo.ca).

The authors are with the Department of Electrical & Computer Engineering, University of Waterloo, 200 University Avenue West, Waterloo, Ontario N2L 3G1, Canada.

$2\pi/2^n$. The beam pointing resolution, $\Delta\theta$, can be found from:

$$\begin{aligned} \frac{2\pi}{2^n} &= k_0 d \sin(\Delta\theta) \\ \Delta\theta &= \sin^{-1}\left(\frac{2}{2^n}\right) \end{aligned} \tag{1}$$

where k_0 is the wave number, and d is the antenna element spacing. Using (1), for a half-wavelength antenna element spacing, the beam pointing resolution of 3-, 4-, and 5-bit digital phase shifters will be 14.5°, 7.2°, and 3.5°, respectively. Since the antenna pointing accuracy for emerging Ka-band satellite communication should be better than 0.2°–0.3°, the required number of bits is at least 9. A 9-bit phase shifter with adequate performance is a complex and costly device. Hence, for extra-fine beam steering, analog phase shifters are preferred because, in principle, they can provide infinite resolution.

From technology standpoint, the existing analog phase shifters can be divided into three general classes: Transmission Line structures (distributed or synthetic), Reflection-Type structures, and Resonance-Based phase shifters.

In Transmission Line (TL) structures, which are often based on coplanar waveguide (CPW line), the phase shifting can be obtained by using varactors, distributed or lumped capacitors, switch lines, or even left-handed transmission lines [9–14]. Adding lumped or distributed capacitance to the transmission lines usually results in low Q-factor (high insertion loss) as well as input impedance mismatch at Ka-band frequencies. Note that the low loss technologies like MEMS based on electromechanical movements will result in larger size non-planar integrated structures. Furthermore, the existing TL phase shifters cannot provide large phase shifting per wavelength, and therefore the transmission line length should be at least a few wavelengths in order to produce 360 degree phase shift. For the transmitter phased array systems, in which the antenna element spacing should be a fraction of wavelength, often there is not enough space to place a TL phase shifter. Hence, we exclude this type of phase shifters in our analysis.

The Reflection Type Phase shifters (RTP) [15–18] use quadrature (hybrid) coupler configurations terminated by reflective loads which are circuits with variable phase reflection characteristics such as shunt capacitors or varactors (when using lumped elements), loaded LC resonators (for larger phase shifts), or a simple quarter wavelength transmission. MEMS and MMIC technologies are commonly used for this type of phase shifters, resulting in compact size structures. However, it should be noted that the phase shift values provided by RTP configurations depend on the reflective load impedance circuit. The reflective load at Ka-band range of frequencies is often a reactive low Q-factor and high loss resonating structure. High quality (low insertion loss) components require large area and therefore not feasible for Ka-band phased array systems, whereas the phase shifter and other element active devices have to be integrated in the feed circuit with a foot print smaller than the array element cell Based on the aforementioned facts RTP is not a suitable candidate as an antenna element integrated phase shifter for Ka-band phased array systems. In addition, the RTP phase frequency nonlinear response highly depends on the resonance behaviour of the utilized reflective impedance circuit.

The Resonance-Based Phase shifters (RBP) use resonating elements whose characteristics are electronically tuned to obtain the required phase shift [19–23]. This type of phase shifter can easily provide 360 degree phase shift with moderate insertion loss, in a compact package size For high performance Ka-band phased array transmitters consisting of very large number of antennas (typically, several thousand elements) with antenna cell size of 5 mm × 5 mm, the Resonance-Based phase shifter is considered as the suitable candidate. In general, among all types of the phase shifters reported in the literature, the Resonance-Based phase shifter is so far a promising solution for generating 360 degree phase shifting in a compact package size or very small circuit area and moderate insertion loss at Ka-band frequencies. However, due to the resonance behaviour of its elements, RBP has nonlinear phase-frequency response, which impacts the phased array antenna performance. The phased array performance degradation due to this nonlinear characteristic is investigated in this paper.

The phase-shifting requirements are dictated by the type of application, bandwidth, and the array architecture and excitation among other factors. Since the beam scanning requirements for satellite communications is the most stringent among other applications, phased-array systems for mobile satellite network is the main focus in this research. Maintaining narrow beamwidth (maximum gain)

and very low side-lobe level over a large angular scanning range, particularly on transmit (uplink) side, is a significant challenge. For a realistic evaluation of the effects of the phase-frequency nonlinear response on the phased-array system, a particular Ka-band array system with optimal excitation coefficients, which has been designed by a new approach developed by the authors, is chosen in this work.

The organization of the paper is as follows. In Section 2, we describe the aforementioned novel approach to synthesize the excitation coefficients of an antenna array whose radiation pattern satisfies the standard satellite communication radiation mask for various beam scanning angles. Detailed and accurate investigation of the effects of nonlinear phase-frequency response of Resonance-Based phase shifters requires rigorous modeling of the behaviour of this class of phase shifters. Therefore in Section 3 we propose a general model for this type of phase shifters. In this section, three kinds of Resonance-Based phase shifters (namely, Chebyshev, Elliptical and All-Pass) are considered. The effects of Resonance-Based phase shifters on phased array system performance will be discussed in Section 4, and finally, the concluding remarks are presented in Section 5.

2. PHASED ARRAY RADIATION PATTERN REQUIREMENTS

One possible strategy to implement phased array antenna is to use multi-panel architecture as presented in [5]. Although multi-panel architecture is a very effective approach, the large distance between the panels (larger than wavelength) results in the grating lobes in the radiation pattern. Note that the grating lobes with substantial large amplitudes will violate the sidelobe envelope mask requirement. To avoid the grating lobes in the multi-panel architecture, the phased array antenna can be implemented in one panel with the element spacing less than half a wavelength. Note that the grating lobe issue is critical for transmitter which MUST meet the standard sidelobe mask, whereas the receiver antenna may violate the sidelobe mask and can still be implemented by multi-panel architecture.

A Taylor/optimization method was proposed in [24] to synthesize the single panel transmitting phased array antenna satisfying the standard mask requirement. Taylor synthesis method is a general approach in which each sidelobe level can be arbitrarily adjusted. Taylor showed that the radiation pattern with the desired sidelobe levels can be synthesized by replacing the nulls of the sinc function with the optimum null positions [25–27]. The nulls can be optimized in such a way that the desired sidelobe levels are achieved. To obtain the optimal null positions, we start with the null positions of the conventional Taylor radiation pattern with a constant sidelobe level. Then, using an iterative perturbation procedure, the optimal null positions which result in the desired radiation pattern are obtained. Once the optimal null positions are known, the current coefficients of antenna elements can be calculated by either the Fourier series or Schelkunoff unit circle [24].

The Ka-band transmitting phased array antenna must meet the radiation mask dictated by FCC 25.209 for earth stations [28]. Also, it is desired to have 40 dBi or higher gain at the main beam direction to provide a certain EIRP (Equivalent isotropically radiated power) required for satellite communications. Using the Taylor/optimization method, the minimum length of transmitting linear array was reported as 40 cm in [24]. Using the Fourier series, the excitation coefficients of antenna elements can be calculated for two perpendicular linear arrays. Having the excitation coefficients of two linear arrays, the current coefficients of 2D array elements can be obtained by multiplying the corresponding coefficients in two linear array antennas. The synthesized current excitations of the planar array are illustrated in Fig. 1(a) for approximately 5000 antenna elements with the spacing of 0.5λ at 29.75 GHz (~ 0.5 cm). Although the presented array synthesis assumes no mutual coupling between the antenna elements, it should be noted that the mutual coupling can be significantly reduced by adding grounding vias around the antenna elements in order to suppress the surface waves propagating through the antenna substrate.

In order to obtain practical excitation coefficients for antenna elements, the calculated coefficients are quantized in 0.5 dB steps and antenna elements with excitation coefficients values less than -10 dB are removed in Fig. 1(a). When using a dual-feed patch antenna as a circularly polarized element, Fig. 1(b) illustrates the corresponding gain pattern of the Tx planar array with the size of 40 cm $\times$ 40 cm for $\varphi = 0^\circ$ and $\varphi = 90^\circ$ planes. As can be observed, the designed planar array can meet the gain and sidelobe envelope requirements. Note that removing the edge elements alleviates the sidelobes and provides a reasonable margin for practical implementation.

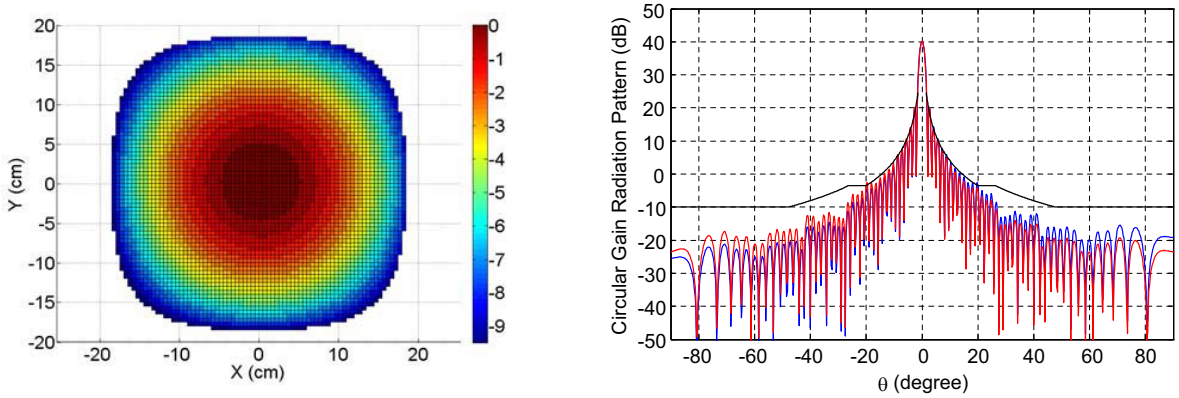

Figure 1. (a) Quantized current coefficients of antenna elements in terms of dB, (b) gain radiation pattern of Tx planar array for practical coefficients.

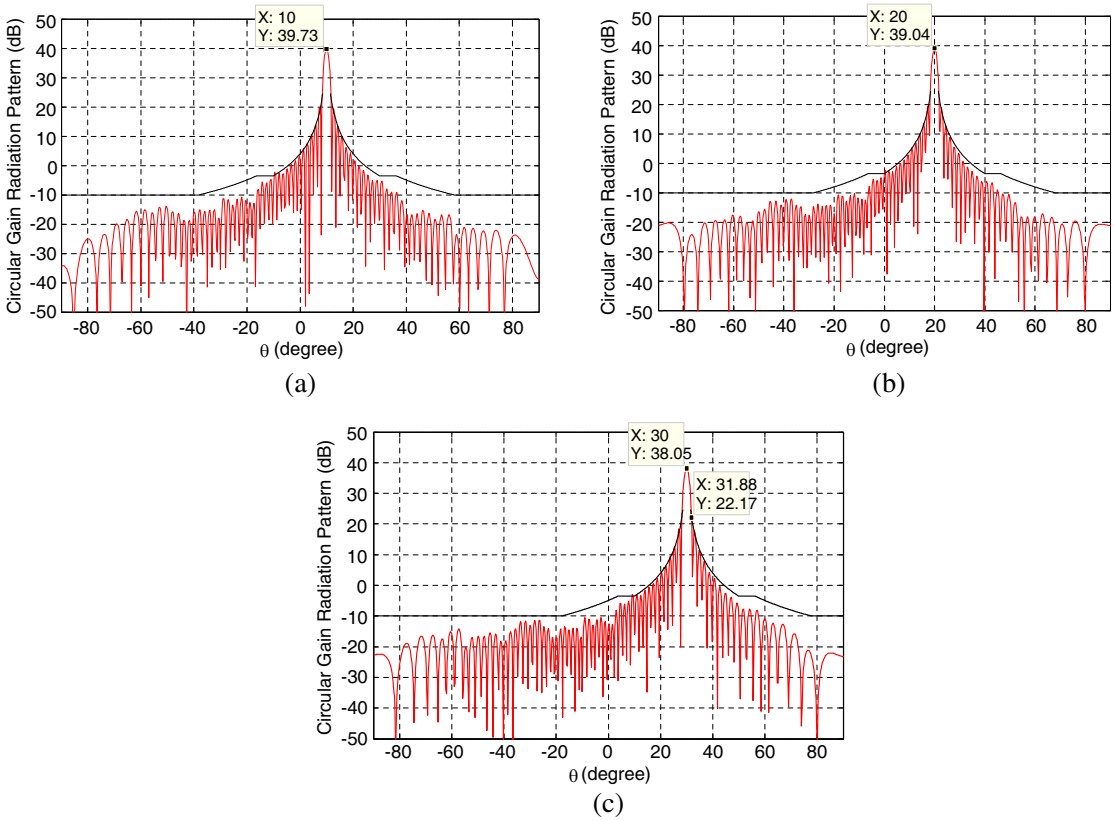

Figure 2. Gain radiation patterns of 40 cm × 40 cm Tx phased array for beam positions of (a) 10°, (b) 20°, and (c) 30°.

Figure 2 shows the gain patterns of the designed 40 cm × 40 cm planar array, when the beam direction is electronically positioned at 10°, 20°, and 30°, respectively. It should be emphasized that, due to the significant gain degradation at larger beam scanning angles, 30° is considered as the maximum electronic beam scanning angle here.

As can be observed, the gain radiation patterns meet the standard sidelobe envelope for various beam scanning angles. However, as expected, the peak gain decreases by 2 dB due to the element

factor degradation and effective aperture area reduction at various beam positions. The resultant gain degradation causes the main beam broadening. For instance, in the case of 30° beam scanning angle, the main beam is broadened by 0.4°.

For the beam steering angles shown in Fig. 2, the ideal analog phase shifters are used, and consequently, it is possible to adjust the required phase shifting for each antenna element. Although the insertion loss variations of phase shifters can significantly affect the antenna gain and radiation patterns as investigated in [29], it is possible to integrate a variable gain amplifier (VGA) with phase shifters [30] in order to compensate loss variations. Having an intelligent element with variable phase and amplitude provides the ability to compensate any amplitude and phase imbalances in the Ka-band components and feed circuits. Accordingly, the amplitude and phase required for each antenna element can be calculated to obtain the radiation patterns illustrated in Fig. 2 for different beam scanning angles. However, the amplitude and phase adjustments are often performed only for the centre frequency, without accurate examination of the phase-shift variation over the entire range of frequencies.

In the next section, an analytical model is presented for Resonance-Based phase shifters to analyze the phase-frequency response nonlinearity over the frequency band of the Tx phased array system (29.5–30 GHz).

3. RESONANCE-BASED PHASE SHIFTERS

For Ka-Band applications, Resonance-Based phase shifters are based on tunable resonance circuits which can be divided into two general classes of Band-Pass and All-Pass circuits. The phase-frequency response depends on the particular design strategy and the characteristics of the tuning mechanism used in the Resonance-Based phase shifter. In the following subsections, a new and comprehensive methodology is presented to investigate the non-linear phase-frequency characteristic of these two types of phase shifters. The methodology here is general and can be applied to a wide range of Resonance-Based response profiles and tuning devices or media, leading to an optimal design in terms of bandwidth and phase-frequency response linearity.

3.1. Band-Pass Phase Shifters

Band-Pass Phase Shifters [20–22] are essentially tunable Band-Pass circuits in which the centre frequency is shifted, resulting in the phase change of the output signal. The maximum centre frequency shift should be adjusted in such a way that the system bandwidth (29.5–30 GHz) is contained in all shifted pass-bands. Fig. 3 illustrates the pass-bands for the lowest, middle, and highest centre frequencies.

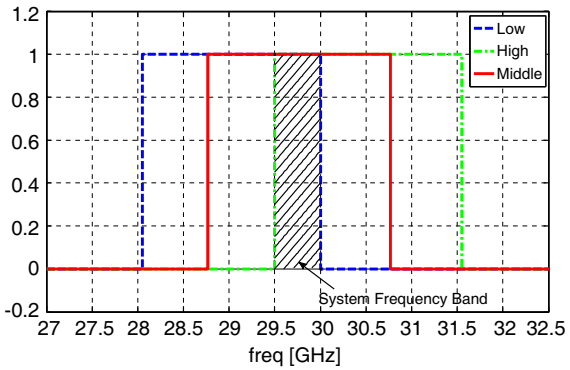

Figure 3. Pass-bands for the lowest, middle, and highest centre frequencies.

An optimal Resonance-Based phase shifter should meet the following criteria:

1) The system bandwidth is contained in all shifted pass-bands.
2) 360 degree phase shifting is obtained over the entire system bandwidth.
3) The required bandwidth should be realizable with a minimum order profile.

An iterative method can be used to determine the minimum order and the required bandwidth for this class of Resonance-Based phase shifters. In the case of the Ka-band system under consideration, the minimum required order and the bandwidth for a Chebyshev band-pass circuit, satisfying all of the above criteria, are obtained as 5 and 2 GHz, respectively. For this bandwidth and the centre frequency of $f_0 = 29.75$ GHz, two band-edge frequencies of the resonance circuit are calculated as [31]:

$$\frac{f_0}{BW}\left(\frac{f}{f_0} - \frac{f_0}{f}\right) = \pm 1 \rightarrow f^2 \mp BW f - f_0^2 = 0 \tag{2}$$

Using (2), the band-edge frequencies of the circuit are obtained as $f_{\text{low}}^{\text{response}} = 28.767$ GHz and $f_{\text{high}}^{\text{response}} = 30.767$ GHz. The circuit type determines the pass-band profile. Fig. 4 illustrates the S-parameters of this resonance circuit with a return loss of 10 dB, and $Q_u = 200$ [31]. As expected, the maximum linearity of the phase response occurs between the calculated $f_{\text{low}}^{\text{response}}$ and $f_{\text{high}}^{\text{response}}$ (Fig. 4(b)). The details of the aforementioned iterative method depend on the physical mechanism of tunability. In an important class of tuneable circuits, the circuit tunability and pass-band shifting are practically achieved by changing the electromagnetic parameters of the tuneable medium used in the circuit structure. Liquid Crystals (LC) and Barium Strontium Titanate (BST) $Ba_xSr_{1-x}TiO_3$ are two common tuneable materials whose dielectric constants are changed by applying an adjustable voltage (applied electric field).

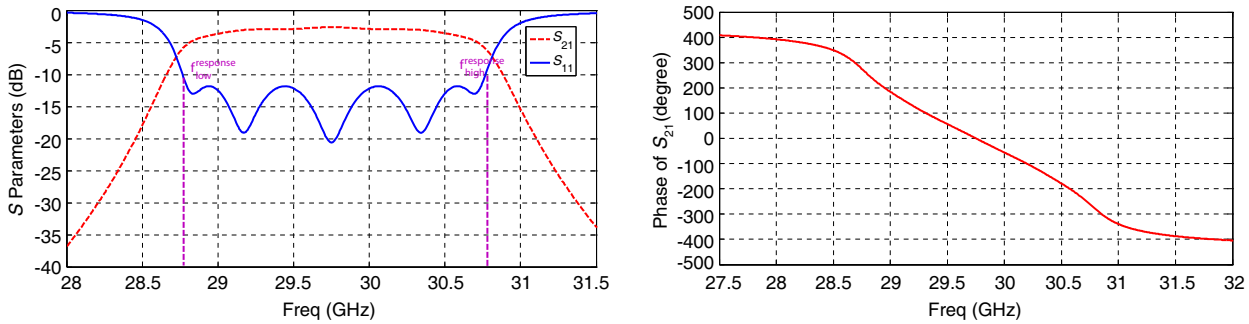

(a) (b)

Figure 4. S parameters of the sample Chebyshev 2 GHz 5-poles circuit with 10 dB return loss and $f_0 = 29.75$ GHz, (a) magnitude and (b) phase response.

The propagation constant, β, and the characteristic impedance, Z_0, change with dielectric constant as well. Hence, the change in material constants not only shifts the centre frequency, but also affects β and Z_0. This latter, however, may not be exactly a desired outcome. To achieve a more realistic model, β and Z_0 variations due to the pass-band shifting have been taken into consideration. Variations of the other parameters such as Bandwidth and Q_u have also been accounted for. It is noted that, in a network made of transmission line segments when the dielectric constant changes, β changes accordingly and the centre frequency as well as the pass-band edges vary by the same ratio.

The proposed iterative method is now presented for band-pass circuits. In the first step, starting with the initial estimate of the bandwidth (typically 4 or 5 times the system bandwidth), two extreme frequency shifts are calculated for the desired circuit characteristics, shown in Fig. 4, in terms of the band-edge frequencies, $f_{\text{low}}^{\text{response}}$ and $f_{\text{high}}^{\text{response}}$. Based on the aforementioned criteria, the maximum frequency shifts of the resonance circuit occur when the band-edge frequencies of two shifted pass-bands approach the side frequencies of phased array system, $f_{\text{low}}^{\text{system}}$ and $f_{\text{high}}^{\text{system}}$ (29.5 and 30 GHz). Accordingly, the centre frequencies of the shifted pass-bands for the ith iteration, namely $f_{0i\,\text{shifted}}^{\text{high}}$ and $f_{0i\,\text{shifted}}^{\text{low}}$, are obtained as follow:

$$\begin{aligned} f_{0i\,\text{shifted}}^{\text{high}} &= f_0 \frac{f_{\text{low}}^{\text{system}}}{f_{\text{low}}^{\text{response}}} \\ f_{0i\,\text{shifted}}^{\text{low}} &= f_0 \frac{f_{\text{high}}^{\text{system}}}{f_{\text{high}}^{\text{response}}} \end{aligned} \tag{3}$$

The total range of phase shift due to centre frequency shift of the band-pass circuit is then calculated. If the phase shift range is less than the desired value (more than 360 degrees), the pass band is increased and the above steps are repeated until the desired phase shift range can be realized.

For the response shown in Fig. 4(a), the optimal range of centre frequencies is calculated as $f_{0\,\mathrm{opt}}^{\mathrm{high}} = 30.508\,\mathrm{GHz}$ and $f_{0\,\mathrm{opt}}^{\mathrm{low}} = 29.008\,\mathrm{GHz}$. For these two shifted pass-band centre frequencies, the S-parameters are plotted in Fig. 5. As can be observed in Fig. 5(a), the shifted responses provide a smooth pass-band for entire system bandwidth (29.5–30 GHz).

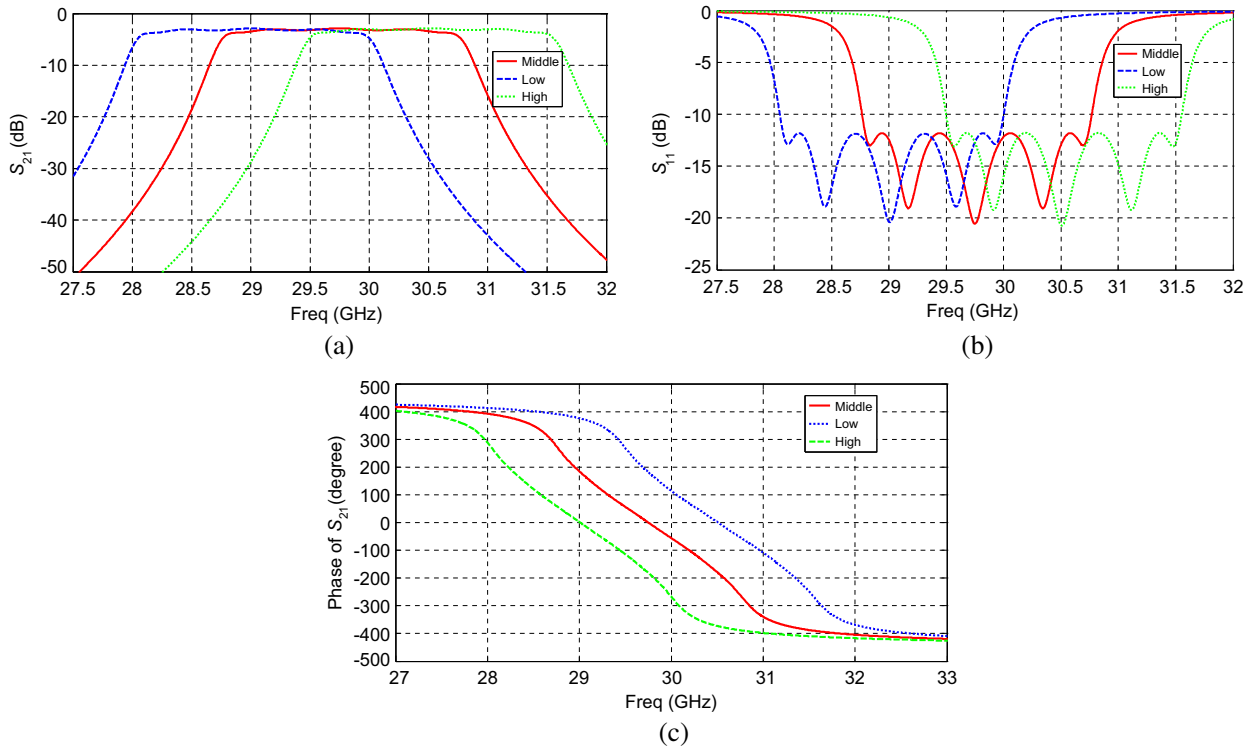

Figure 5. (a) Magnitude of S_{21}, (b) magnitude of S_{11}, and (c) phase response S_{21} for the shifted response at shifted centre frequencies (f_0, $f_{0\,\mathrm{opt}}^{\mathrm{high}}$ and $f_{0\,\mathrm{opt}}^{\mathrm{low}}$).

Note that the smooth pass-band is attributed to the fact that the response ripple is largely reduced by the finite Q_u of the circuit resonators at Ka-band frequencies. Having such a smooth pass-band is one of the other advantages of Resonance-Based phase shifters as compared to other types. Also, note that the phase shifting process is performed in the linear part of phase response, which has been shown in Fig. 4(b). Hence, the wide-band circuits with wider linear phase region are preferred. However, in general, practical implementation of wide-band circuits is not challenging.

Figure 6 demonstrates the phase response of the above mentioned circuit within the phased array system frequency band (29.5–30 GHz) for two extreme and middle state phase shifts. As can be seen, more than 360 degree phase shift is obtained. Although the difference between phase-frequency plots, corresponding to various phase shift states, is reasonably constant near the centre frequency, certain variations are observed as band-edges are approached. The effect of these variations on the phased array performance is discussed in Section 4.

The same procedure can be applied to any other types of band-pass circuits including Elliptical circuits with required amplitude/phase characteristics. Elliptical circuits provide a smaller range of phase shift as compared with the Chebyshev circuits due to existence of Transmission Zeros in their transfer function. Therefore, in order to obtain more than 360° phase shift, a larger number of poles or wider bandwidth is required for Elliptical circuits. The dual-mode ring resonator circuit [19] is an example of Elliptical circuits which has been used as a Ka-band phase shifter.

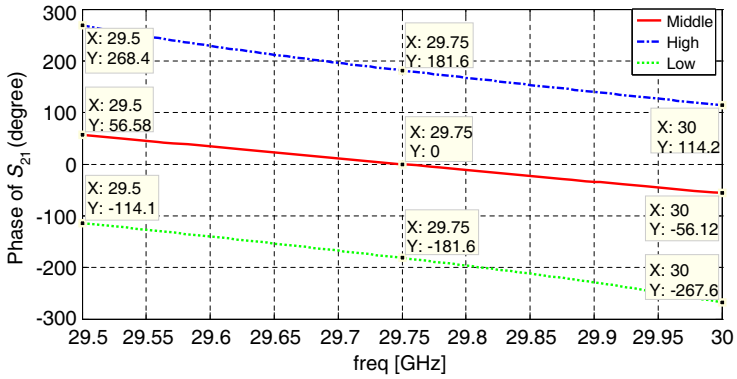

Figure 6. Phase response of circuits in shifted centre frequencies (f_0, $f_{0\,\mathrm{opt}}^{\mathrm{high}}$ and $f_{0\,\mathrm{opt}}^{\mathrm{low}}$).

3.2. All-Pass Phase Shifters

All-Pass circuit is another type of resonance circuits commonly used to realize Resonance-Based phase shifters [23, 32]. In this Section, an approach similar to the one described in Section 3.1, is applied to All-Pass circuits. The difference is that the All-Pass circuits theoretically provide an infinite bandwidth, and consequently, the first criterion mentioned in previous Section is relaxed. Although All-Pass circuits practically provide a finite bandwidth, the available bandwidth is still large enough to justify ignoring the first criterion. Since All-pass circuits have flat amplitude response for all frequencies, the linearity of the phase response is used as a criterion for the phase shifter bandwidth in the proposed iterative method. As a linearity criterion, the variation of the phase response slope should be as small as possible.

After the iterative procedure, outlined in the previous section, was applied, it is observed that the 2nd order All-Pass circuits can provide 360 degree phase shifting over the system bandwidth (29.5–30 GHz). According to the transfer function of a 2nd order All-Pass circuit [33]

$$H(s) = \frac{s^2 - 2\sigma_b s + s_b^2}{s^2 + 2\sigma_b s + s_b^2}, \quad s_b^2 = \sigma_b^2 + \omega_b^2 \tag{4}$$

the zeros and poles are located symmetrically with respect to imaginary axis. Hence, for the same variation of the centre frequency and the same pole locations as those in Chebyshev circuits, the phase shift obtained from All-Pass circuit is expected to double. This is the reason why a 2nd order All-Pass circuit (2 poles and 2 zeros) can achieve more than 360° total phase shift. The phase of (4) is:

$$\sphericalangle H(s) = -2\left\{\tan^{-1}\left(\frac{\omega - \omega_b}{\sigma_b}\right) + \tan^{-1}\left(\frac{\omega + \omega_b}{\sigma_b}\right)\right\} \tag{5}$$

The linearity of the phase response is dependent on the position of poles and zeros of the resonance circuit ($-\sigma_b \pm j\omega_b$, $\sigma_b \pm j\omega_b$) in the complex plane [33]. ω_b, σ_b should be optimized based on the required phase-frequency response linearity and the maximum phase shifting. It should be noted that the linear phase response bandwidth can be increased by reducing ω_b, and increasing σ_b. For the particular system requirements under consideration in this paper, our designed values are $\sigma_b = 24$ and $\omega_b = 26$. To perform phase shifting, tuneable materials are used to change the location of poles and zeros, which yields into shifting the phase-frequency response. As indicated earlier, the extreme cases where maximum shifting occurs are limited by the obtained linearity bandwidth and the maximum material tunability. Fig. 7 and Fig. 8 show the phase response of 2nd order All-Pass circuit with the chosen parameters for two extreme and the middle phase shift states.

In the following section, we will investigate the effects of phase-frequency response nonlinearity of three Resonance-Based phase shifters (Chebyshev, Elliptical and All-Pass) on the performance of the phased array system.

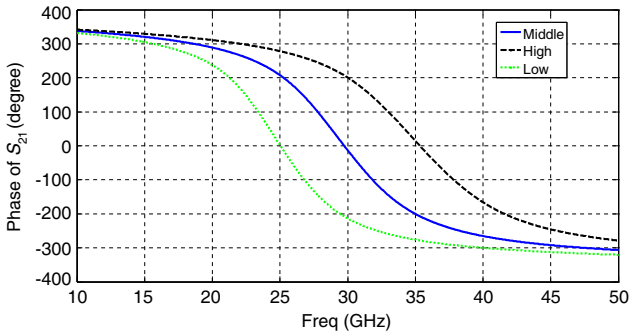

Figure 7. Phase response of the typical 2nd order All-Pass circuit.

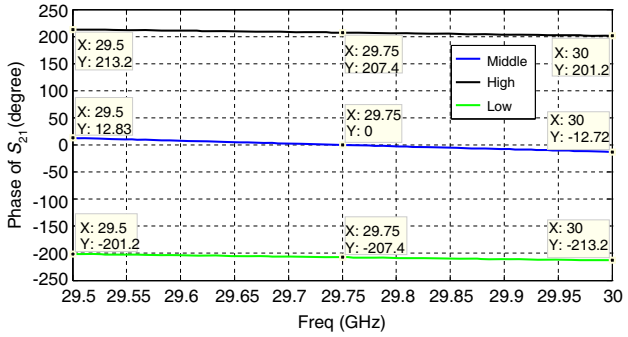

Figure 8. Phase of S_{21} over the system bandwidth for the typical 2nd order All-Pass circuit.

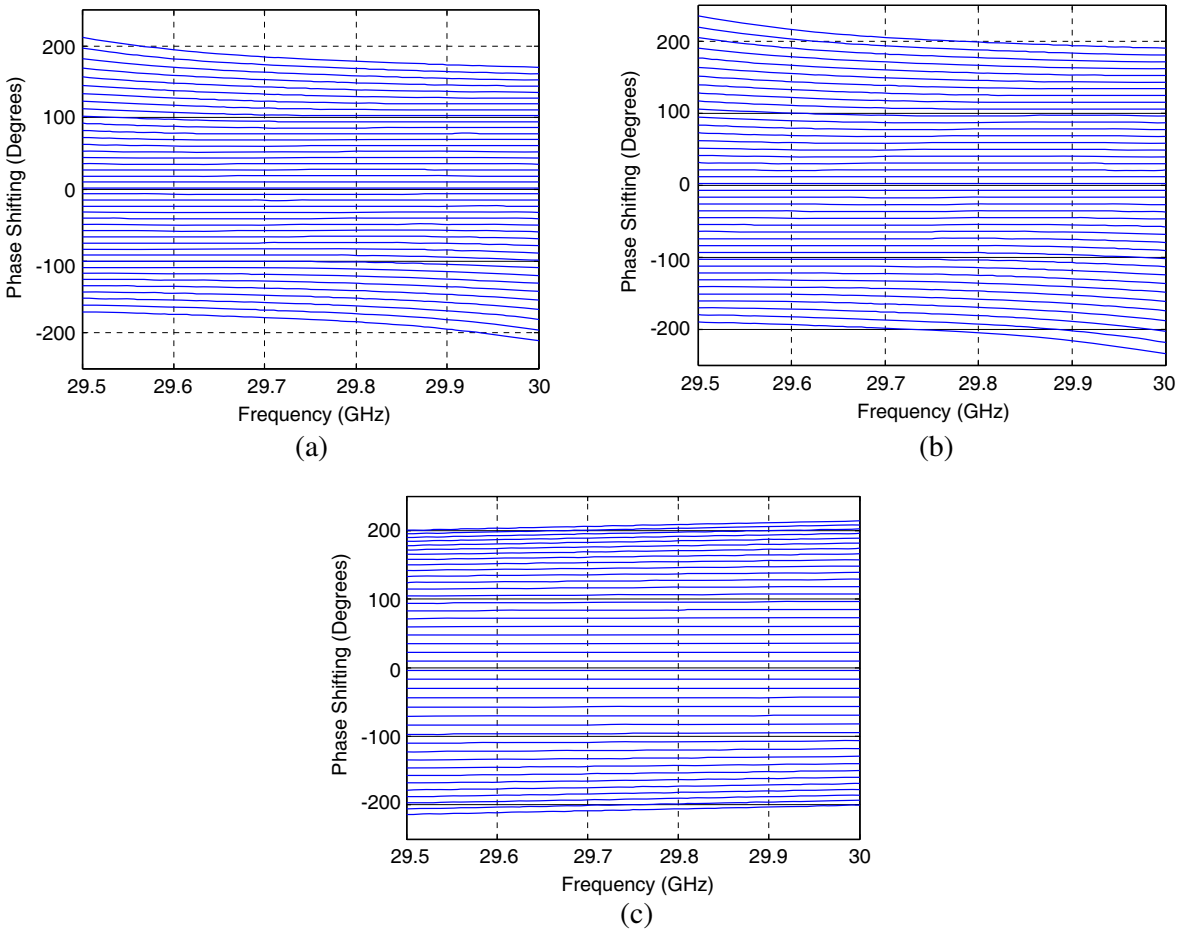

Figure 9. The phase shifting of three types of phase shifters versus frequency, (a) Chebyshev with the order of 5, the return loss of 10 dB, the bandwidth of 2 GHz, and Q_u equal to 200, (b) Elliptical with the order of 6, the return loss of 10 dB, the bandwidth of 2 GHz, and Q_u equal to 200, and (c) 2nd order All-Pass circuit ($\sigma_b = 24$, $\omega_b = 26$).

4. THE EFFECTS OF PHASE-FREQUENCY NONLINEARITY ON THE PERFORMANCE OF THE PHASED ARRAY SYSTEM

In the transmitter phased array considered here, each antenna element is equipped with a VGA and a phase shifter. The initial phase and amplitude for each antenna element are adjusted such that the synthesized radiation patterns shown in Fig. 4 are realized at the centre frequency (29.75 GHz). Using the phase shifter modeling presented in Section 3, the effects of nonlinear phase-frequency responses of three different (Chebyshev, Elliptical, and All-Pass) phase shifters on the phased array radiation pattern and the main beam gain in the scanned direction are studied.

In Fig. 9, the phase shifter models outlined in Figs. 6 and 8 have been extended and detailed for the three aforementioned phase shifters. Each curve corresponds to a particular voltage applied to the phase shifter structure. Note that the relative phase shifts are plotted with respect to the phase response of the middle state. Hence, the phase shifts of the middle state are assumed to be zero at all frequencies.

For a particular beam direction, the phase shift required for each antenna element can be calculated and the suitable voltage commands are applied to all phase shifters to realize those phase shifts at 29.75 GHz (centre frequency). This will result in the desired radiation patterns illustrated in Fig. 2 for various beam scanning angles at 29.75 GHz. However, the applied voltages provide the calculated phase shifts only at 29.75 GHz, and the relative phase shift at other frequencies will deviate from those of the ideal case at the centre frequency.

Using the realistic phase shifter behavioural models of Fig. 9, the maximum phase shift error occurs at the lowest and highest frequencies (29.5 GHz and 30 GHz). The gain radiation patterns at 29.5 GHz, 29.75 GHz, and 30 GHz, obtained from the realistic phase shifter models (Fig. 9), are shown in Figs. 10, 11, and 12 for various beam scanning angles. Figs. 10–12 show that the phase-frequency response nonlinearity of various phase shifters can significantly affect the side lobes and cause critical violation of radiation mask. Hence, once the applied voltages are adjusted for the centre frequency, the relative

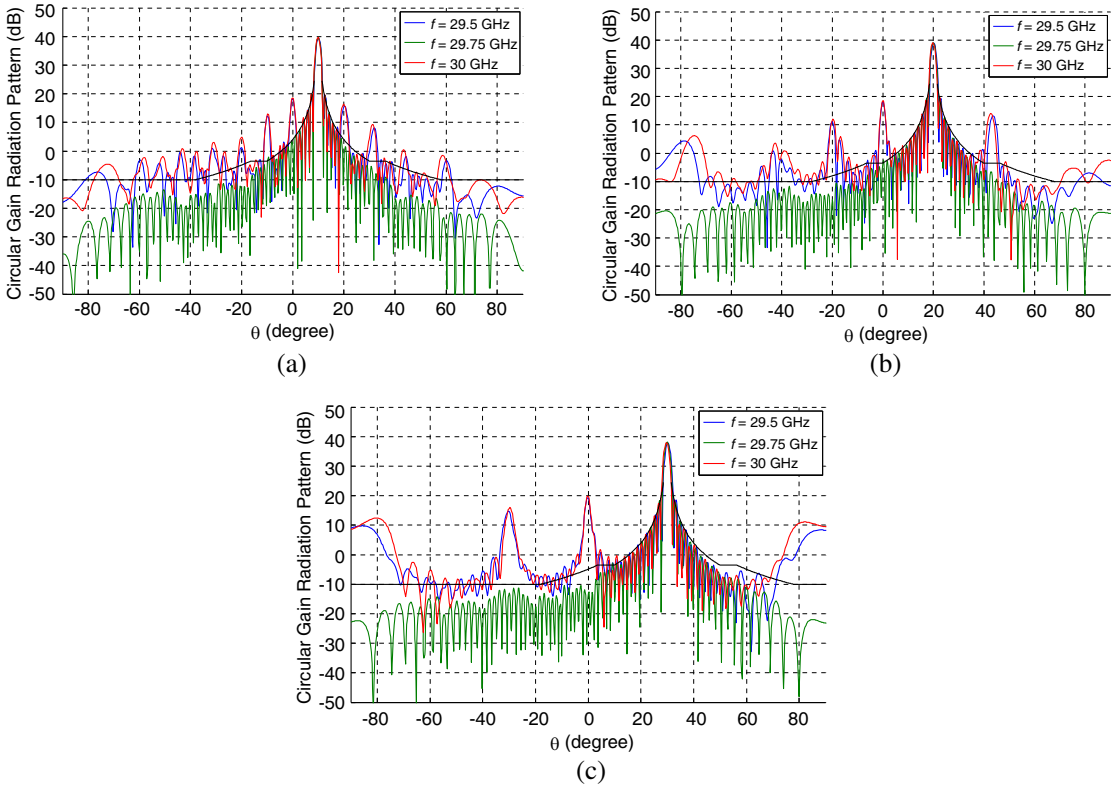

Figure 10. Gain radiation pattern at $f = 29.5$, 29.75, and 30 GHz for Chebyshev phase shifter when the scanning angle is (a) 10°, (b) 20°, (c) 30°.

phase shift errors at other frequencies have led to mask violation. It can also be observed that the mask violation is more critical at larger scanning angles, which require larger phase shifts.

Comparing the radiation patterns obtained by different types of phase shifters, one can conclude that the mask violation is less critical in the case of 2nd order All-Pass phase shifters. This is due to the fact that All-Pass phase shifters can provide a linear phase-frequency response over a wider range of frequencies. However, the mask violation is still critical for larger scanning angles.

4.1. Distortion Due to Phase Shifter Non-Linearity

In addition to the mask violation, the phase-frequency response nonlinearity will result in the beam positioning errors. In Fig. 13, the angular region close to the main beam maximum of Fig. 11(c) has been expanded. As shown, the main beam is deviated from the desired beam direction (30°). The deviation angle is frequency-dependent. Fig. 14 depicts the phased array gain versus frequency for various phase shifter types and different desired scanning angle. As expected, the gain variations over the frequency band increase for larger scanning angles. Table 1 presents the maximum gain variations for various types of resonance circuits and different beam scanning angles.

The curves presented in Fig. 14 characterize the phased array system distortion. Once the distortion effect is known, the amplitude imbalances at different frequencies can be compensated through pre-distortion techniques in both RF and digital domains. Thus, the presented analysis can be employed to compensate the phase shifter phase-frequency response nonlinearities.

4.2. Phased Array System Bandwidth Considerations

It is shown in [34] that, depending on the employed signal modulation method, error correction coding scheme, and multiple access option, for a 300 Mbps data stream, the required bandwidth for each

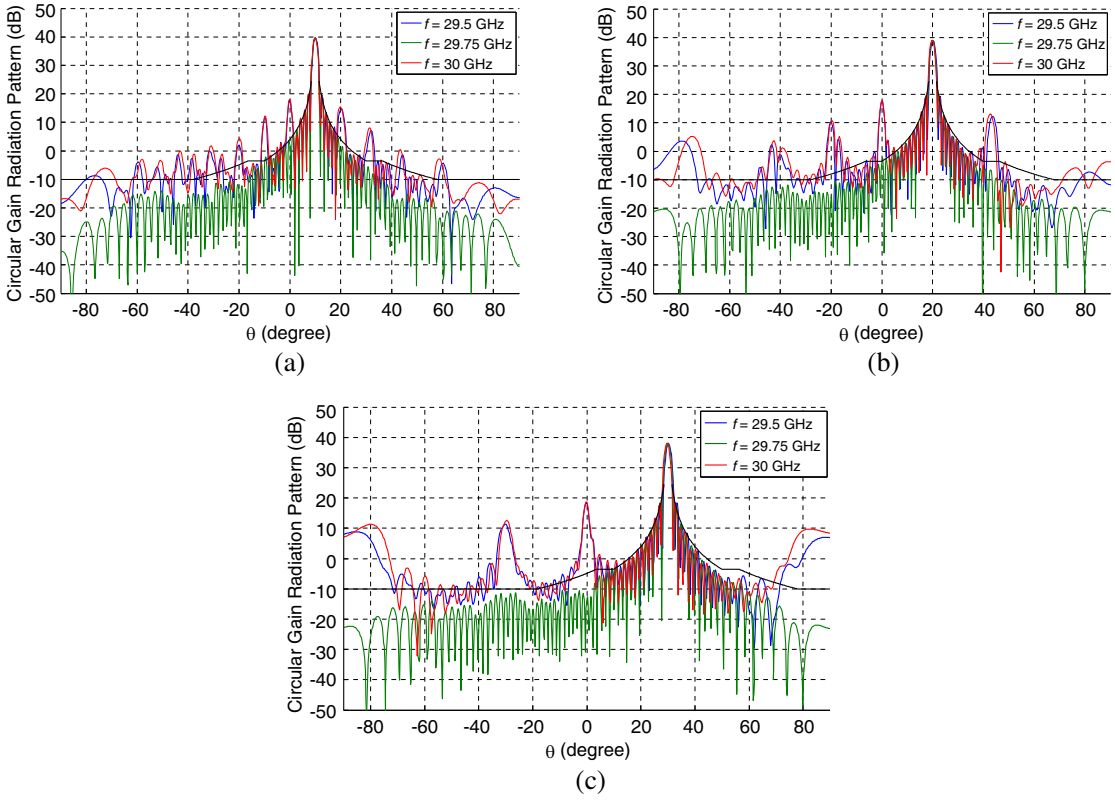

Figure 11. Gain radiation pattern at $f = 29.5$, 29.75, and 30 GHz for Elliptical phase shifter when the scanning angle is (a) 10°, (b) 20°, (c) 30°.

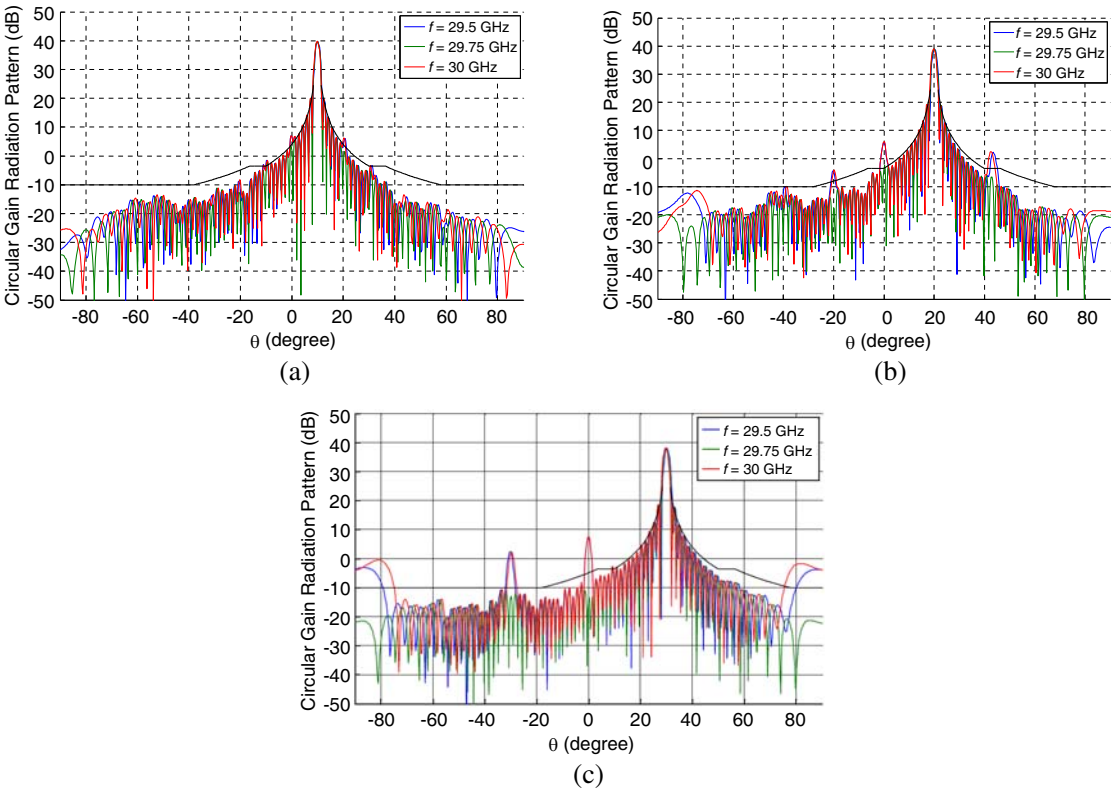

Figure 12. Gain radiation pattern at $f = 29.5$, 29.75, and 30 GHz for All-Pass phase shifter when the scanning angle is (a) 10°, (b) 20°, (c) 30°.

Table 1. Maximum gain variation over the frequency for Chebyshev, Elliptical, and All-Pass phase shifters and various beam scanning angles.

	Chebyshev	**Elliptical**	**All-Pass**
10°	0.18 dB	0.17 dB	0.14 dB
20°	0.27 dB	0.26 dB	0.20 dB
30°	0.51 dB	0.43 dB	0.34 dB

terminal would vary between 150 MHz–300 MHz (spectral efficiency of 1 to 2). Here, we demonstrated that in addition to vital trade-offs discussed in [34], for phased array terminals, another important limitation on the system bandwidth comes from phase shifter phase-frequency response non-linearity. The presented simulation results show that the type of phase shifters used in the phased array system can significantly affect the radiation patterns at scanned beam position. Among the Resonance-Based phase shifters considered here, the All-Pass phase shifter has shown less non-linear effects due to its wide bandwidth linear phase-frequency response. However, the mask violation is still critical at the system band edges. By limiting the system bandwidth, it is possible to meet the standard mask requirement for all the frequencies. Fig. 15 depicts the gain radiation patterns of phased array antenna at 29.685 GHz, 29.75 GHz, and 29.815 GHz for the largest beam scanning angle (30°).

The radiation patterns shown in Fig. 15 meet the standard radiation mask requirement. Note that the mask violation at $\theta = -30°$ is less than 3 dB which is acceptable according to FCC 25.209 which states "For θ greater than 7 degrees, the envelope may be exceeded by no more than 10% of the sidelobes, provided no individual sidelobe exceeds the given gain envelope by more than 3 dB" [28]. Therefore, for particular phase shifter designs investigated in this paper and a maximum scanning angle of 30°, the system bandwidth, satisfying the standard mask, is limited to 130 MHz. Depending on the spectral

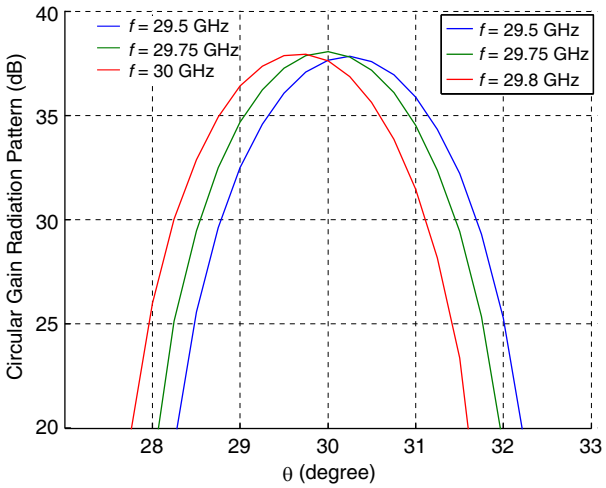

Figure 13. Beam positioning error at $f = 29.5$, 29.75, and 30 GHz for the case of Elliptical phase shifter when the scanning angle is 30°.

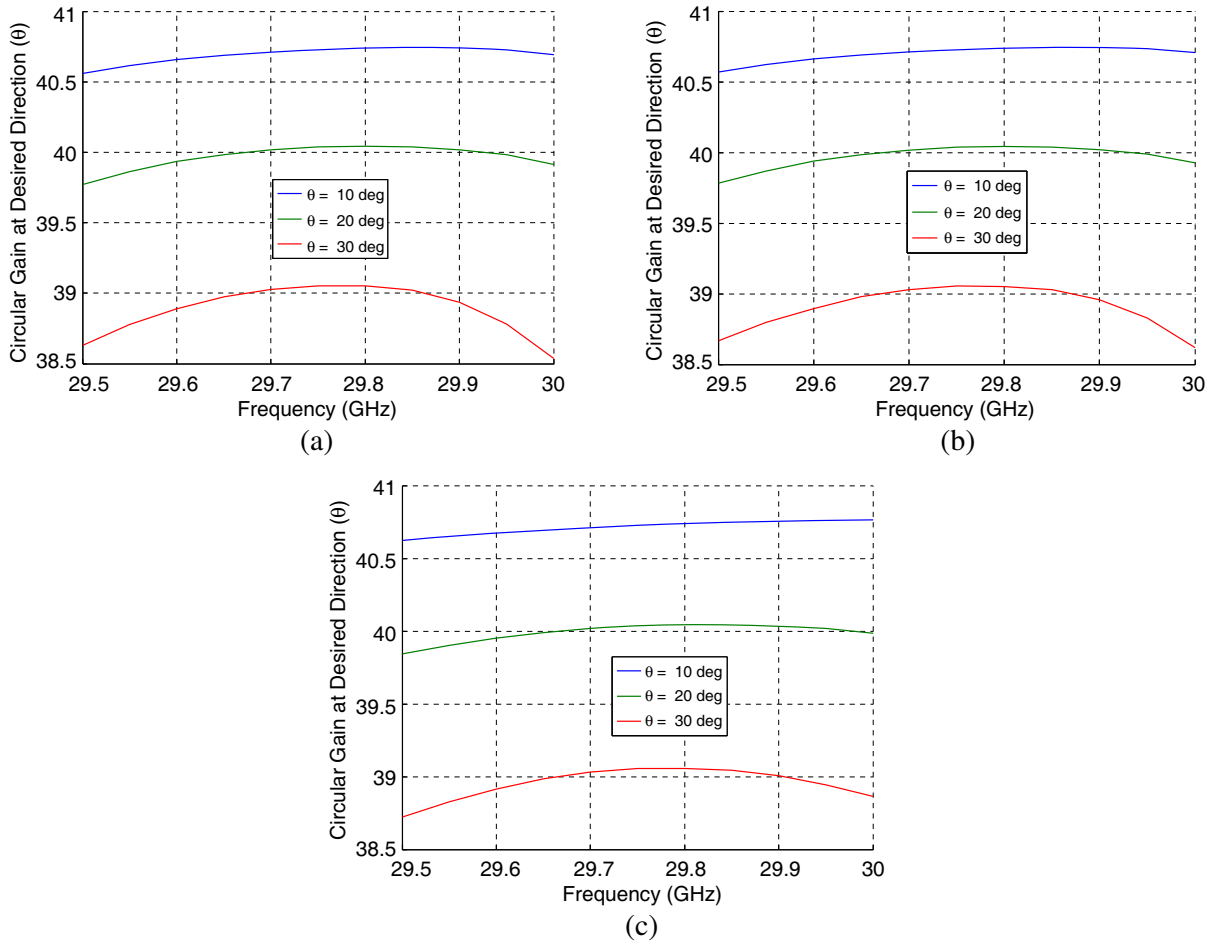

Figure 14. Transmitting Gain versus frequency for beam scanning angles of 10°, 20°, and 30° when using (a) Chebyshev, (b) Elliptical, and (c) All-Pass phase shifters.

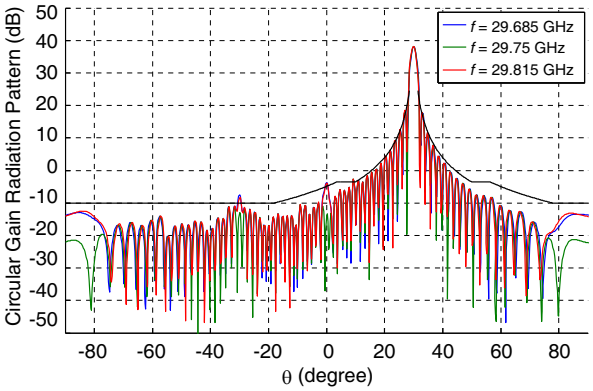

Figure 15. Gain radiation pattern at $f = 29.685$, 29.75, and 29.815 GHz for All-Pass phase shifter when the scanning angle is 30°.

efficiency of the chosen physical layer (typically between 1 to 2), the maximum achievable system data rate varies between 130–260 Mbps.

5. CONCLUSIONS

In this paper, the effects of the phase shifter phase-frequency response nonlinearities on the radiation pattern, gain, and the beam pointing direction of the phased array systems are investigated using an effective analytical modeling along with an iterative method for Resonance-Based phase shifters. Using optimal designs in the analysis, the paper presented a realistic assessment for the impact of the phase-frequency non-linear response on performance of a phased array system. In particular, the method was successfully applied to a Ka-band phased array system for satellite communications. Using the developed analytical models and proposed design procedures, it was shown that the radiation mask can be significantly violated over the system bandwidth. Therefore, in addition to other system requirements, the dispersion created by phase shifter phase-frequency response nonlinearity imposes an important limitation on the phased array system bandwidth. The phase shifter response nonlinearity can also generate transmitted signal amplitude distortion. The analytical modelling and the presented analysis can rigorously characterize the dispersion/distortion effects related to nonlinear phase-frequency responses which can be included in the waveform design for radio communications using phased array systems.

ACKNOWLEDGMENT

This work has been supported by NSERC (Natural Sciences and Engineering Research Council) of Canada, OCE (Ontario Centres of Excellence) of Canada, C-COM Satellite System Inc. (Ottawa, Canada), and BlackBerry (former RIM).

REFERENCES

1. Ozbay, C., W. Teter, D. He, M. J. Sherman, G. L. Schneider, and J. A. Benjamin, "Design and implementation challenges in Ka/Ku dual-band Satcom-On-The-Move terminals for military applications," *MilCOM*, 2006.
2. Stark, A., et al., "SANTANA: Advanced electronically steerable antennas at Ka-band," *3rd European Conference on Antennas and Propagation, EuCAP 2009*, 471–478, Mar. 2009.
3. Jung, Y.-B., S. Eom, S. Jeon, A. V. Shishlov, and C. Kim, "Novel hybrid antenna design having a shaped reflector for mobile satellite communication applications," *IEEE AP-S Int. Symp.*, Toronto, Canada, Jul. 2010.

4. Kang, D.-W., J.-G. Kim, B.-W. Min, and G. M. Rebeiz, "Single and four-element-band transmit/receive phased-array silicon RFICs with 5-bit amplitude and phase control," *IEEE Transactions on Microwave Theory and Techniques*, Vol. 57, No. 12, 3534–3543, Dec. 2009.
5. Fakharzadeh, M., S. H. Jamali, P. Mousavi, and S. Safavi-Naeini, "Fast beamforming for mobile satellite receiver phased arrays: Theory and experiment," *IEEE Trans. Antennas Propagat.*, Vol. 57, No. 6, 1645–1654, Jun. 2009.
6. Imaizumi, Y., Y. Suzuki, Y. Kawawkami, and K. Arakia, "A study on an onboard Ka-band phased-array-fed imaging reflector antenna," *2002 IEEE APS*, 144–147, 2002.
7. Rock, J. C., T. Hudson, B. Wolfson, D. Lawrence, B. Pillans, A. R. Brown, and L. Coryell, "A MEMS-based, Ka-band, 16-element sub-array," *2009 IEEE Aerospace Conference*, 1–11, Big Sky, MT, Mar. 2009.
8. Greda, L. A. and A. Dreher, "Tx — Terminal phased array for satellite communication at Ka-band," *2007 EuMC*, 2007.
9. Nagra, A. S. and R. A. York, "Distributed analog phase shifters with low insertion loss," *IEEE Transactions on Microwave Theory and Techniques*, Vol. 47, 1705–1711, Sep. 1999.
10. Rebeiz, G. M., G.-L. Tan, and J. S. Hayden, "RF MEMS phase shifters: Design and applications," *IEEE Microwave Mag.*, Vol. 3, 72–81, Jun. 2002.
11. Erker, E. G., A. S. Nagre, Y. Liu, P. Periaswamy, T. R. Taylor, J. Speck, and R. A. York, "Monolithic Ka-band phase shifter using volatge tunable $BaSrTiO_3$ parallel plate capacitors," *IEEE Microwave Guided Wave Lett.*, Vol. 10, 10–12, 2000.
12. Bulja, S. and D. Mirshekar-Syahkal, "Meander line millimetre-wave liquid crystal based phase shifter," *Electronics Letters*, Vol. 46, No. 11, 769–771, 2010.
13. Sazegar, M., et al., "Compact tunable phase shifters on screen-printed BST for balanced phased arrays," *IEEE Transactions on Microwave Theory and Techniques*, Vol. 59, No. 12, 3331–3337, 2011.
14. Sokolov, V., et al., "A Ka-band GaAs monolithic phase shifter," *IEEE Transactions on Microwave Theory and Techniques*, Vol. 31, No. 12, 1077–1083, 1983.
15. Ashtiani, A. E., et al., "Monolithic Ka-band 180-degree analog phase shifter employing HEMT-based varactor diodes," *IEE Colloquium on Microwave and Millimetre-wave Oscillators and Mixers*, No. 480, 1998.
16. Abbosh, A. M., "Compact tunable reflection phase shifters using short section of coupled lines," *IEEE Transactions on Microwave Theory and Techniques*, Vol. 60, No. 8, 2465–2472, 2012.
17. Miyaguchi, K., et al., "An ultra-broad-band reflection-type phase-shifter MMIC with series and parallel LC circuits," *IEEE Transactions on Microwave Theory and Techniques*, Vol. 49, No. 12, 2446–2452, 2001.
18. Lambard, T., et al., "A novel analog 360° phase shifter design in Ku and Ka bands," *Microwave and Optical Technology Letters*, Vol. 52, No. 8, 1733–1736, 2010.
19. Moessinger, A., et al., "Compact tunable Ka-band phase shifter based on liquid crystals," *2010 IEEE MTT-S International Microwave Symposium Digest*, 2010.
20. Walters, R. A., et al., "Tunable end-coupled ferroelectric-gap filters based on barium strontium titanate capacitors," *IEEE Asia-Pacific Conference on Applied Electromagnetics, 2005, APACE 2005*, 2005.
21. Abadei, S., A. Deleniv, and S. Gevorgian, "Filter-phase shifters based on thin film ferroelectric varactors," *34th European Microwave Conference, 2004*, Vol. 3, 2004.
22. Deleniv, A., S. Abadei, and S. Gevorgian, "Tunable ferroelectric filter-phase shifter," *2003 IEEE MTT-S International Microwave Symposium Digest*, Vol. 2, 2003.
23. Ni, N. and A. H. Cardona, "Ku-band analog phase shifters using individually designed all-pass networks with BST tunable capacitors," *2011 IEEE Radio and Wireless Symposium (RWS)*, 2011.
24. Mohajer, M., Gh. Z. Rafi, and S. Safavi-Naeini, "A taylor synthesis/optimization method for 2D minimum size transmitting phased array antenna," *IEEE AP-S Int. Symp.*, Orlando, Florida, USA, Jul. 2013.

25. Elliott, R. S., *A Classic Reissue: Antenna Theory and Design*, Revised Edition, IEEE and Wiley, New York, 1981.
26. Elliot, R. S., "Design of line-source antennas for sum patterns with sidelobes of individually arbitrary heights," *IEEE Trans. Antennas Propagat.*, Vol. 24, 76–83, Jan. 1976.
27. Taylor, T. T., "Design of line-source antennas for narrow beamwidth and low sidelobes," *IRE Trans. Antennas Propagat.*, Vol. 3, 16–28, 1955.
28. FCC 25.209, "Antenna performance standards," Revised as of Dec. 4, 2012.
29. Fakharzadeh, M., P. Mousavi, S. Safavi-Naeini, and S. H. Jamali, "The effects of imbalanced phase shifters loss on phased array gain," *IEEE Antennas Wireless Propag. Lett.*, Vol. 7, 192–196, Jul. 2008.
30. Min, B.-W. and G. M. Rebeiz, "Single-ended and differential-band BiCMOS phased array front-ends," *IEEE J. Solid-State Circuits*, Vol. 43, No. 10, 2239–2250, Oct. 2008.
31. Matthaei, G. L., L. Young, and E. M. T. Jones, *Microwave Filters, Impedance-matching Networks, and Coupling Structures*, Vol. 5, McGraw-Hill, New York, 1964.
32. Viveiros, D., Jr., D. Consonni, and A. K. Jastrzebski, "A tunable all-pass MMIC active phase shifter," *IEEE Transactions on Microwave Theory and Techniques*, Vol. 50, No. 8, 1885–1889, 2002.
33. Hong, J. G. and M. J. Lancaster, *Microstrip Filters for RF/Microwave Applications*, Vol. 167, Wiley.com, 2004.
34. Blanco, M. A. and M. N. Richard, "Waveform design for Ka-band SATCOM high data rate links," Technical Paper, The MITRE Corporation, Oct. 2006.